Article **Journal of Chemical and Physical Energy**
June 2023, Vol.10 No.28 1-7

Physical properties of Ag_3SbS_3 thin films for photovoltaic applications

Propiedades físicas de películas delgadas de Ag_3SbS_3 para aplicaciones fotovoltaicas

GARCÍA-GUILLÉN, Grisel*†, GONZÁLEZ-GARZA, Jorge Oswaldo and RÍOS, Bernardino

Universidad Politécnica de García

ID 1st Author: *Grisel, García-Guillén* / **ORC ID**: 0000-0002-5919-7755, **CVU CONAHCYT ID**: 297209

ID 1st Co-author: *Jorge Oswaldo, González-Garza* / **ORC ID:** 0000-0002-98212-6947, **CVU CONAHCYT ID**: 248626

ID 2nd Co-author: *Bernardino, Ríos* / **ORC ID**: 0009-0007-6254-1223, **CVU CONAHCYT ID**: 329047

DOI: 10.35429/JCPE.2023.28.10.1.7 Received March 10, 2023; Accepted June 30, 2023

Abstract

Ag_3SbS_3 thin films have been prepared by heating multilayers of glass/Sb_2S_3/Ag at different temperatures. Thin film of Sb_2S_3 were deposited on glass substrates using chemical bath deposition technique. Thermal evaporation of silver followed by annealing at 300 and 350°C were carried out to synthetize Ag_3SbS_3 thin films. XRD spectra showed the formation of Ag_3SbS_3 thin films at 300 and 350 °C with a micro-strain and grain size of 1.8 x 10^{-3} and 21 nm, respectively. Electrical conductivity in the range of 10^{-4} – 10^{-5} $(\Omega cm)^{-1}$ and a band gap of 1.3 eV were obtained.

Thin films, Semiconductor, Absorber material, Chemical bath deposition, Thermal evaporation, Formation, Substrate, Conductivity

Resumen

Películas delgadas de Ag_3SbS_3 fueron sintetizadas por tratamiento térmico de multicapas de vidrio/Sb_2S_3/Ag a diferentes temperaturas. La película delgada de Sb_2S_3 fue depositada por la técnica de baño químico. Una capa de Ag fue depositada por evaporación térmica y después se sometieron las multicapas a tratamiento térmico a 300°C y 350°C, respectivamente. Los patrones de difracción confirman la formación de películas delgadas de Ag_3SbS_3 para ambas temperaturas de tratamiento térmico, mostrando una micro-deformación de 1.8 x 10^{-3} nm y un tamaño de grano de 21 nm. Se reporta una conductividad eléctrica en el rango de 10^{-4} – 10^{-5} $(\Omega cm)^{-1}$ y una brecha de energía prohibida de 1.3 eV.

Película delgada, Semiconductor, Material absorbedor, Baño químico, Evaporación térmica, formación, Substrato, Conductividad

Citation: GARCÍA-GUILLÉN, Grisel, GONZÁLEZ-GARZA, Jorge Oswaldo and RÍOS, Bernardino. Physical properties of Ag_3SbS_3 thin films for photovoltaic applications. Journal of Chemical and Physical Energy. 2023. 10-28:1-7

* Correspondence to the Author (e-mail: grisel@upgarcia.edu.mx)
† Researcher contributing as first author

1. Introduction

Research of novel materials for energy production and storage have recently made significant progress and are on track toward developing alternative energy sources. Metal chalcogenide thin films have attracted attention in recent years due their potential applications in opto-electronic and photovoltaic devices (Alharbi, Alam, Salhi, Missous, & Lewis, 2021). Photovoltaic (PV) solar cells are semiconductor-based devices that convert sunlight energy into electricity. One of the components of the solar cell device is absorber material, which converts the incident sunlight photon energy into electricity.

The most used absorber material is Si due to its high efficiency (>20%) and good reliability (<25 years). However, there are emerging photovoltaic absorber materials, such as SnS, Sb_2Se, Cu_2SnS_3, $CuSbSe_2$ and $AgSbS_2$, which are made with more environmentally friendly and earth-abundant elements (Zakutayev, 2017) (Nadukkandy, et al., 2021) (Alharbi, Alam, Salhi, Missous, & Lewis, 2021). Ag_3SbS_3 is a novel absorber material that crystallizes in a monoclinic structure having a high absorption coefficient of 10^5 cm^{-1} in the visible range with bang gap around 1.8 eV, depending on the deposition conditions (Thanabalan, Johnson, Kannusamy, & Ganesan, 2016) (Thanabalan, S. Thangaraj, Kannusamy, & Ganesan, 2019). Ag_3SbS_3 thin films have been prepared by different methods such as thermal evaporation, hydrothermal method, etc. (Thanabalan, S. Thangaraj, Kannusamy, & Ganesan, 2019) (Tubtimtae, Huang, Shi, & Lee, 2016). Antimony sulfide (Sb_2S_3) thin films were deposited by chemical bath deposition (Vinayakumar, et al., 2018), then other layers were deposited by heating chemical precursors in order to obtain ternary chalcogenide thin films for photovaltaic and photodetection applications (Nadukkandy, Shaji, Avellaneda Avellaneda, Aguilar-Martínez, & Krishnan, 2023).

This research work is focused on Ag_3SbS_3 thin films prepared by heating multilayers of glass/Sb_2S_3/Ag deposited by chemically deposited Sb_2S_3 followed by thermally evaporated Ag thin films, due to there are no reports using this material and its optoelectronical properties can be suitable for photovaltaic applications.

2. Materials and Method

2.1 Deposition of Sb_2S_3 thin films

Sb_2S_3 thin films were deposited on 7.5 x 2.5 cm clean glass substrates by chemical bath deposition technique. The chemical bath deposition was prepared using 0.650 g of $SbCl_3$, then it was dissolved in 2.5 ml of acetone using a 100 ml beaker, followed by the addition of 25 ml of 1M Na_2SO_3 and 72.5 ml of preheated deionized water (40 °C), then the solution was stirred for 30 seconds. Finally, the solution was used to fill a Petri dish containing clean glass substrates placed horizontally and the chemical bath was maintained at 40°C for 1 hour. The chemical bath deposition was made twice resulting in a uniform orange Sb_2S_3 thin films of ~ 500 nm of thickness. The thickness was measured using a confocal microscope (ZEISS, Axio CSM 700).

2.2 Deposition of Ag thin films

A silver layer of 70 nm was deposited by thermal evaporation on Sb_2S_3 thin film. Silver wire of 99.999 % purity was evaporated onto glass/Sb_2S_3 layers at high vacuum using a high vacuum system (INTERCOVAMEX-TE12P) and its thickness was measured using a quartz crystal thickness monitor.

2.3 Heat treatment

The multilayers of glass/Sb_2S_3/Ag were heated at two different temperatures, samples M1 and M2 at 300°C and 350°C, respectively, for 1 hour at low vacuum (10-3 torr) in a vacuum furnace (TM Vacuum products model No V/IG-803-14).

2.4 Characterization

X-ray diffraction patterns of the samples were recorded by PANalytical diffractometer using Cu Ka1 radiation with λ = 1.54059 Å. The scan range (2θ) was from 10° to 70°. Morphological studies were done using scanning electron microscope FEI Nova NanoSEM 200 associated with an Energy Dispersive X-ray detector (EDX), the optical transmittance and specular reflectance were recorded using a Shimadzu 3600 spectrophotometer, electrical measurements were carried out using Keithley 6487 Picoammeter/Voltage source interfaced with a computer.

ISSN: 2410-3934

For the DC conductivity measurements, the contacts used were two planar electrodes of 3 mm in length and 3 mm in separation using carbon paint.

3. Results

3.1 X-ray Diffraction

Graph 1 and Graph 2 show the XRD spectra for samples heated at 300 °C (M1) and 350 °C (M2), respectively. For both samples can be observed well defined peaks at 2θ positions 27.7°, 28.78°, 30.97°, 32.26°, 32.71°, that corresponds to the planes (041), (-102), (-122), (-202) and (-212) which match the standard pattern of Ag_3SbS_3 (JCPDS #25-1187). Additionally, traces of unreacted Sb_2S_3 are observed. The presence of secondary phases can be attributed to not enough temperature for the antimony and sulfide atoms to diffuse and completely react, or the Ag layer thickness was not enough and acts as a limiting reagent.

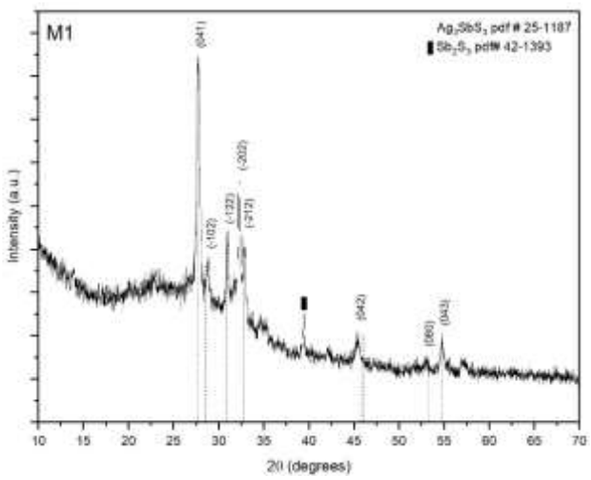

Graph 1 XRD patterns of Ag_3SbS_3 thin films heated at 300°C for 1 h in vacuum

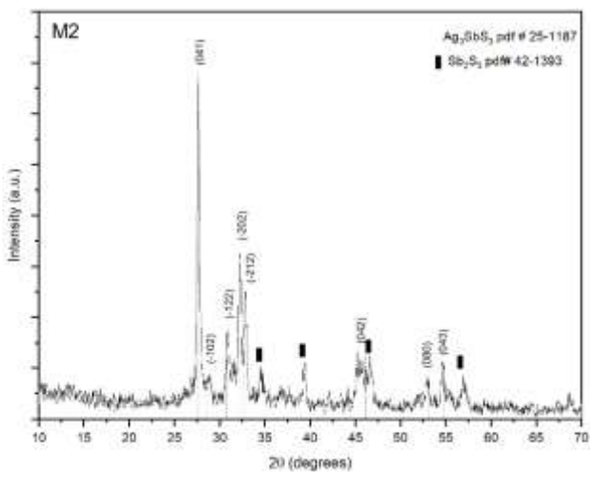

Graph 2 XRD patterns of Ag_3SbS_3 thin films heated at 350°C for 1 h in vacuum

The average crystallite size of the Ag_3SbS_3 thin films was evaluated using the line broadening analysis of the diffraction patterns. The diffraction peak broadening can be attribute to small crystallite size as well as micro-strain present in the films (Tubtimtae, Huang, Shi, & Lee, 2016). The average crystal size was determined using the Scherrer´s formula (Jebali, Khemiri, & Kanzari, 2016):

$$D = \frac{0.9x\lambda}{\beta x \cos\theta} \quad (1)$$

Where D is the average crystallite size, λ is the X-ray wavelength, θ is the diffraction angle of the stronger peak and β is the full width at half maximum (FWHM). The micro-strain ε was evaluated by using the equation (Jebali, Khemiri, & Kanzari, 2016):

$$\varepsilon = \frac{\beta \cos\theta}{2} \quad (2)$$

Sample M1 (300°C) showed an average crystallite size of 21 nm and a micro-strain ε of 1.73 x 10^{-3}, and the sample M2 (350°C) showed an average crystallite size of 25 nm and a micro-strain ε of 1.43 x 10^{-3}. The increase in the average crystallite size can be due to the coalescence of small grains by grain boundary diffusion, that is a thermal activated process, which results in the formation of bigger grains. Also, it is observed a reduction in micro-strain as the temperature in increased from 300°C to 350 °C, this indicates an improvement in the crystalline quality of the films (Jebali, Khemiri, & Kanzari, 2016).

3.2 Morphology

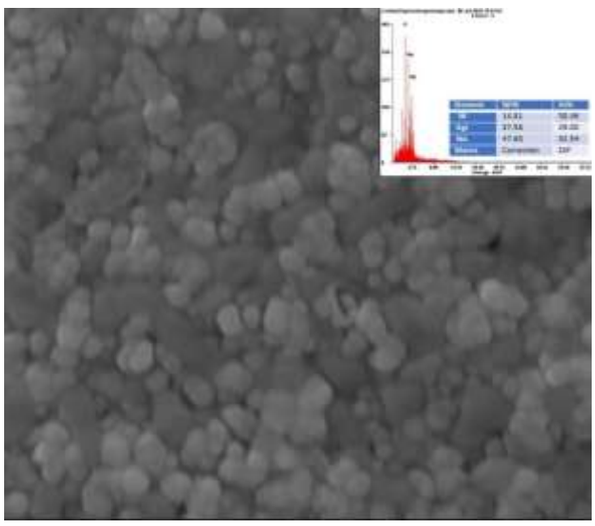

Figure 1 Scanning electron micrograph of glass/Sb_2S_3/Ag multilayers heated at 350°C for 1 h in vacuum

ISSN: 2410-3934

Figure 1 depics the scanning electron micrography at 50,000X for the multilayers heated at 350 °C for 1h. The surface morphology of the fimls showed a compact structure with interconected grains, and no pin holes were observed. The EDX was taken at different areas of the surface of the thin films, the results showed an homogeneous surface distribution of the elements with weigth percentage of 14.81%, 37.58%, and 47.6% for S, Ag and Sb, respectively.

3.3 Optical Properties

Optical transmission (%T) and reflection (R%) of samples M1 and M2 were recorded in the wavelength range of 200 - 1100 nm. Graph 3 shows the optical absorption coefficient of the Ag_3SbS_3 thin films, that was computed using the following relation (González, et al., 2013):

$$\alpha = \left(\frac{1}{d}\right) Ln\left[\frac{(1-R^2)}{T}\right] \quad (3)$$

where R and T are the specular reflectance and optical transmittance, respectively, and d is the film thickness which was ~ 600 nm for both samples. From Graph 3, it is observed high absorption coefficients between $1x10^4$ and $1x10^5$ cm^{-1} in the visible range, which make this material a suitable candidate as absorber in heterojuction photovoltaic structures.

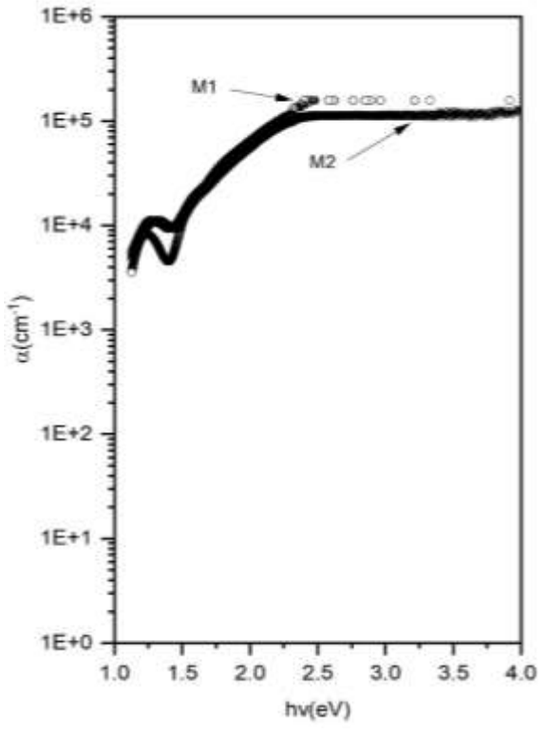

Graph 3 Absorption coefficient of Ag_3SbS_3 thin films heated at 300°C and 350°C

Graph 4 shows the optical band gaps for samples heated at 300°C and 350 °C, labeled as M1 and M2, respectively. The band gap of the samples was calculated using the following formula (González, et al., 2013):

$$(\alpha hv)^n = A(hv - E_g) \quad (4)$$

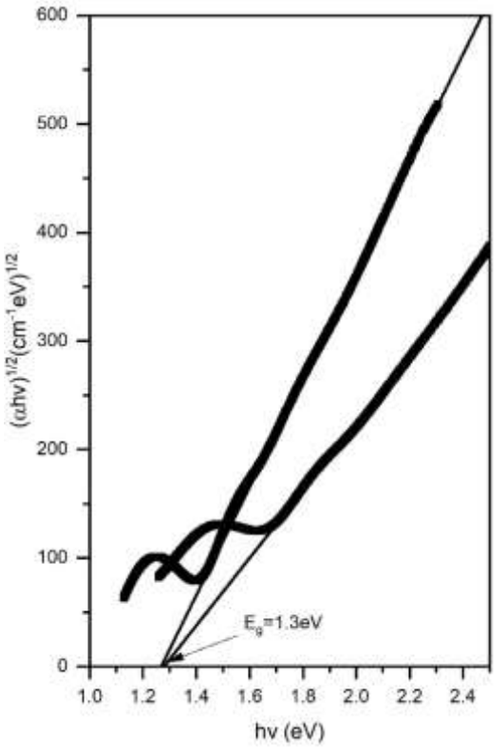

Graph 4 Tauc plots of Ag_3SbS_3 thin films heated at 300°C and 350°C

where α is the absorption coefficient, h is the planck´s constant, v is the frecuency, A is a constant, E_g is the optical band gap and n can take values of 2, 1/2, 2/3 for allowed direct, allowed indirect, and forbidden optical transitions, respectively. The Tauc plot shown in Graph 4 of $(\alpha hv)^n$ vs hv for both samples has a good linear fit when n = 1/2, that implies that the fundamental absorption of Ag_3SbS_3 thin films is dominated by an indirect allowed transition. By extrapolating the linear fit to α = 0, the value of the bang gap was estimated as 1.3 eV for both samples.

3.4 Electrical Properties

Graph 5 shows the photocurrent response of Ag_3SbS_3 thin films. The ohmic behavior of the carbon contacts was verified by a potential sweep and the corresponding current measurement, showing a straight line, given in the inset of the graph.

ISSN: 2410-3934

To measure the photo-current, a bias voltage of 100 V for sample M1 and 20 V for sample M2 was applied and the current was measured through the sample as follows: 10 s in dark, 20 s under illumination and 10 s after switching off the illumination, respectively. Sample heated at 300 °C showed a dark conductivity ~ 10^{-5} $(\Omega cm)^{-1}$ and sample heated at 350 °C showed a value ~ 10^{-4} (Ωcm^{-1}). The increase in dark conductivity can be attributed to the bigger grain size of sample heated at 350 °C and can be explained as follows: as long as the grain size increases, the grain boundaries are reduced, and the mobility of the charge carriers increases by reducing the trapping sites at grain boundaries (Jong Hoon Lee, 2015). Hot probe tests on the samples showed p-type conductivity. P-type conductivity of Ag_3SbS_3 is due to the presence of defects of Ag or Sb vacancies (VAg or VSb) (González, et al., 2013).

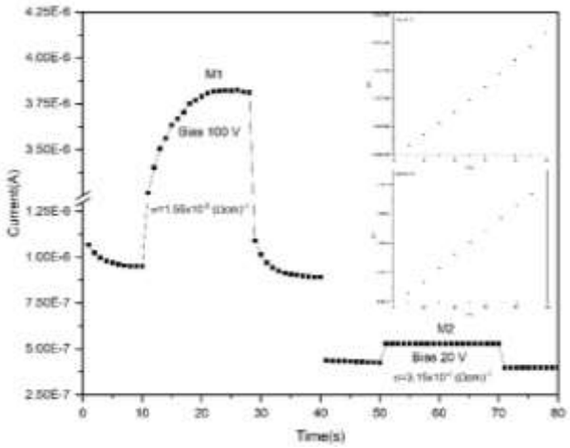

Graph 5 Electrical properties of multilayers of glass/Sb_2S_3/Ag heated at 300°C and 350°C

4. Discussion

One portion of the hypothesis proposed was to obtain a ternary Ag-Sb-S material by promoting crystal grain growth using thermal treatment conditions, which is expected to achieve better optical and electrical properties due to a decrease in the grain boundaries of the material. In the XRD study, the diffraction pattern corresponds to the material Ag_3SbS_3 (Rhomboedral, a=, b=, c=) in the Graph 1 and Graph 2, it was observed greater intensity in planes (041), (-102), (-122), (-202) and (-212). The crystallization improves as the temperature of the thermal treatment increases and the appearance of the ternary compound Ag_3SbS_3 for both samples (M1 & M2) is found, providing further evidence of Ag incorporation into Sb_2S_3.

In the morphology study, the calculation of D for the M1 sample was 21 nanometers and for M2 sample was 25 nanometers, an increase of 4 nanometers indicates an improvement in the crystallinity quality of the material.

It was observed by XRD study that Ag is incorporated on the Sb_2S_3 thin film leading a decrease in the electrical resistivity of the material with electrical conductivity values obtained in the order of 10^{-5} – 10^{-4} $(\Omega cm)^{-1}$ as well as on band gap value with E_g = 1.3 eV compared to other materials such as Sb_2S_3 of E_g = 1.88 eV, being an ideal candidate for applications in solar cells.

However, for future work is proposed to carry out the study for different thermal treatments to improve crystallization and grain size increasing of the Ag_3SbS_3 materials and its application in solar cells.

5. Conclusions

Ag_3SbS_3 thin films were prepared by heating multilayers of glass/Sb_2S_3/Ag at 300°C and 350°C under vacuum. XRD showed the formation of Ag_3SbS_3 as a major phase and traces of unreacted Sb_2S_3. Morphology studies depicted compact structures with no pin holes and uniform distribution of the element in the samples. Optical measurements showed high absorption coefficients ~ 10^4 – 10^5 cm^{-1} in the visible range and indirect allowed transitions with a band gap ~ 1.3 eV. Ag_3SbS_3 thin films showed p-type conductivities with values 10^{-5} – 10^{-4} $(\Omega cm)^{-1}$ measured in dark.

Acknowledgement

We want to thank FIME-UANL and Universidad Politecnica de Garcia for letting us do the experiments at its premises.

Funding

This research received no external funding.

ISSN: 2410-3934

References

Alharbi, Y. T., Alam, F., Salhi, A., Missous, M., & Lewis, D. J. (2021). Direct synthesis of nanostructured silver antimony sulfide powders from metal xanthate precursors. *Scientific Reports*, 3053. doi:https://doi.org/10.1038/s41598-021-82446-3. URL:https://www.nature.com/articles/s41598-021-82446-3

González, J., Shaji, S., Avellaneda, D., Castillo, A., Das Roy, T., & Krishnan, B. (2013). AgSb(SxSe1−x)2 thin films for solar cell applications. *Materials Research Bulletin*, 1939-1945. doi: https://doi.org/10.1016/j.materresbull.2013.01.040. URL: https://www.sciencedirect.com/science/article/abs/pii/S0025540813000597.

Jebali, A., Khemiri, N., & Kanzari, M. (2016). The effect of annealing in N2 atmosphere on the physical properties of SnSb4S7 thin films. *Journal of Alloys and Compounds*, 38-43. doi: https://doi.org/10.1016/j.jallcom.2016.02.159. URL: https://www.sciencedirect.com/science/article/abs/pii/S0925838816304261.

Jong Hoon Lee, Y. H. (2015). Grain-size effect on the electrical properties of nanocrystalline indium tin oxide thin films. *Materials Science and Engineering: B*, 37-41. doi:https://doi.org/10.1016/j.mseb.2015.04.011. URL: https://www.sciencedirect.com/science/article/abs/pii/S092151071500135X.

Nadukkandy, A., Devasia, S., Paulosutty, A., Shaji, S., Avellaneda, D., Aguilar-Martínez, J., . . . Krishnan, B. (2021). Monoclinic AgSbS2 thin films for photovoltaic applications: Computation,. *Materials Science in Semiconductor Processing*, 106074. doi:https://doi.org/10.1016/j.mssp.2021.106074. URL: https://www.sciencedirect.com/science/article/abs/pii/S1369800121004194.

Nadukkandy, A., Shaji, S., Avellaneda Avellaneda, D., Aguilar-Martínez, J., & Krishnan, B. (2023). Cubic structured silver antimony sulfide-selenide solid solution thin films for sustainable photodetection and photovoltaic application. *Journal of Alloys and Compounds*, 199072. doi:https://doi.org/10.1016/j.jallcom.2023.169072. URL: https://www.sciencedirect.com/science/article/abs/pii/S0925838823003754.

Thanabalan, D., Johnson, H., Kannusamy, M., & Ganesan, S. (2016). AgSbS2 and Ag3SbS3 absorber materials for photovoltaic applications. *Materials Chemistry and Physics*, 1-7. doi:https://doi.org/10.1016/j.matchemphys.2016.06.077. URL: https://www.sciencedirect.com/science/article/abs/pii/S0254058416304916.

Thanabalan, D., S. Thangaraj, N., Kannusamy, M., & Ganesan, S. (2019). Influence of film thickness variation on the photo electrochemical cell performances of Ag3SbS3 thin films. *Vacuum*, 138-142. doi:https://doi.org/10.1016/j.vacuum.2018.12.031. URL: https://www.sciencedirect.com/science/article/abs/pii/S0042207X18316981.

Tubtimtae, A., Huang, C.-L., Shi, J.-B., & Lee, M.-W. (2016). Ag3SbS3 thin films formedbyannealinghydrothermallysynthesized. *MaterialsLetters*, 58-60. doi:https://doi.org/10.1016/j.matlet.2016.04.165. URL: https://www.sciencedirect.com/science/article/abs/pii/S0167577X16306644.

Vinayakumar, V., Hernández, C., Shaji, S., Avellaneda Avellaneda, D., Aguilar-Martínez, J., & Krishnan, B. (2018). Effects of rapid thermal processing on chemically deposited antimony sulfide thin films. *Materials Science in Semiconductor Processing*, 9-17. doi:https://doi.org/10.1016/j.mssp.2018.02.011. URL: https://www.sciencedirect.com/science/article/abs/pii/S1369800117324654.

ISSN: 2410-3934

Zakutayev, A. (2017). Brief review of emerging photovoltaic absorbers. *Current Opinion in Green and Sustainable Chemistry*, 8-15. doi:https://doi.org/10.1016/j.cogsc.2017.01.002 .URL: https://www.sciencedirect.com/science/article/abs/pii/S245222361630092X.

ISSN: 2410-3934